GEORG-AUGUST-UNIVERSITÄT
GÖTTINGEN

EGU General Assembly 2020

Simulating Climate Change Impacts on the Recharge Dynamics of a Mediterranean Karst Aquifer

EGU General Assembly 2020, Mai 5th, 2020

Lysander Bresinsky[1], Jannes Kordilla[1], Emanuel Thoenes[1], Thibault Würsch[1], Irina Engelhardt[2] and Martin Sauter[1]

[1]University of Goettingen, Applied Geosciences, Goettingen, Germany
[2]Hydrogeology Department, Technische Universität Berlin, Berlin, Germany

- Dualistic flow dynamics in the phreatic zone:
  - Matrix: Low hydraulic conductivity, high storage.
  - Fracture/Conduit: High hydraulic conductivity, low storage.
- Dualistic infiltration dynamics in the vadose zone:
  - Matrix: Diffuse recharge
  - Fracture/Conduit: Focused direct recharge (i.e. preferential flow)

⇒ Continuum Porous Equivalent models often fail to account for this heterogeneity

⇒ Accounting for unsaturated flow crucial for predicting flow

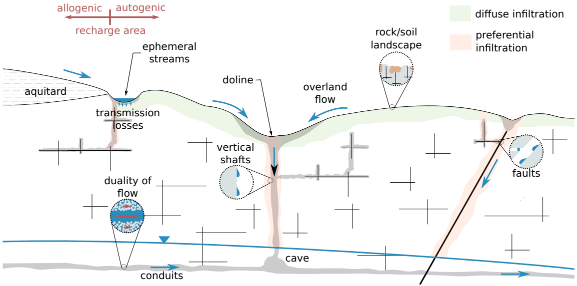

Conceptual model of infiltration into karst rocks (modified after Kordilla et al., 2017; Hartmann et al., 2014).

Project area

- Western Mountain Aquifer (WMA) located in Israel and the Palestinian Territories
- Area: $\sim 9000\,\text{km}^2$
- Semi-arid Mediterranean climate; rainy season from November to April
- Average precipitation of 550 - 600 mm/a
- 330 - 360 MCM/a recharge, $\sim 30-35\%$ of precipitation
- Historically, the aquifer drained towards two springs (Taninim and Yarkon spring)
- Heavy groundwater abstraction led to the drying up of the Yarkon spring in the 1970s

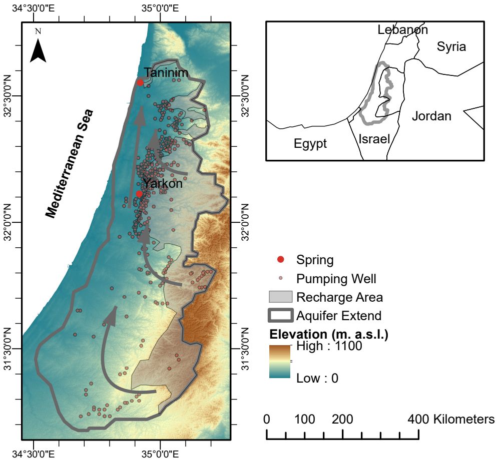

Location map of the Western-Mountain-Aquifer. Arrows indicate the general flow direction.

Hydrogeology of the WMA

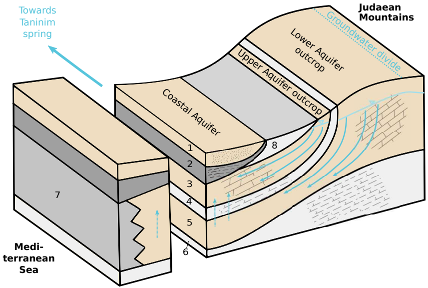

1) Pleistocene Aquifer
2) Saqiye Aquiclude
3) Upper Aquifer
4) Aquitard
5) Lower Aquifer
6) Lower Cretaceous Aquiclude
7) Talme Yafe Group
8) Eocene & Senonian Aquitard

Conceptual illustration of the general hydrogeology (modified after Weinberger et al., 1994).

- Highly karstified and fractured carbonate aquifer (mainly limestone and dolomite)
  - Subdivided into an Upper and Lower Aquifer by Marl of the Moza and Bet Meir Formation.
  - Little interaction with saline Mediterranean waters due to impermeable layers (chalky marls) of the Talme Yafe Formation.
- Groundwater recharge occurs through the exposed rock along the anticline in East
  - Scarce cover of soil
  - Abundant direct exposure of karstic carbonate rock
  - ⇒ Emphasizing focused direct recharge
- Several hundreds meters thick vadose zone

Objectives

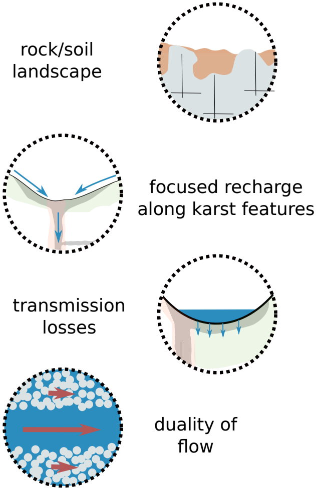

- Estimate groundwater recharge based on a rigorous implementation of the surface-hydrological processes, that accounts for:
    - the particularities of rock-soil landscape,
    - focused recharge along karst features (i.e. sinkholes),
    - transmission losses of ephemeral streams (wadis),
    - specific climate conditions as well as the different precipitation patterns.
- Simulation of the effect of infiltration through a thick (several hundreds of meters) vadose zone on groundwater flow dynamics.

HydroGeoSphere

- HydroGeoSphere (HGS) from Aquanty, Waterloo, Canada utilized as flow simulator
- Dual-continuum representation of the subsurface
    - Variably-saturated flow (Richards' equation)
    - Van-Genuchten Parametrization
- Computation of Overland flow
- Surface-subsurface coupled model
- For the mathematical framework refer to Appendix A.

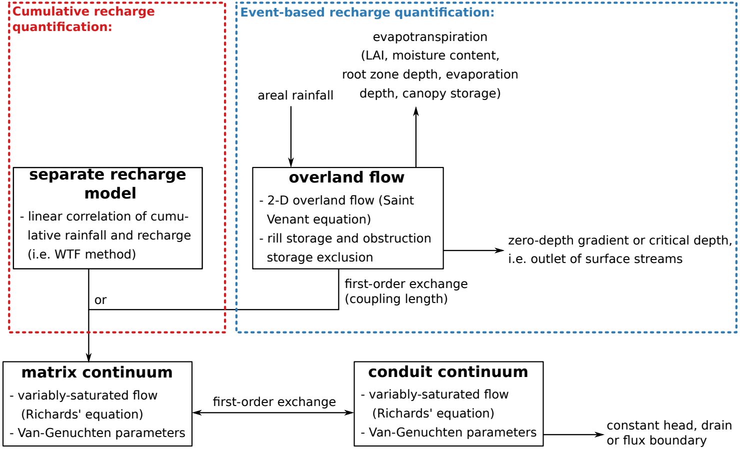

Flow compartments of HGS.

Calibration of variably-saturated dual-continuum flow model

- A variably-saturated dual-continuum model of the WMA has been inversely calibrated based on the hydraulic heads and spring discharge rates (1951 - 2006).
- The simulated discharge reproduces the drying up of the Yarkon spring in the 1970s. The simulation replicates the reactivation (1991/92) of the Yarkon spring.

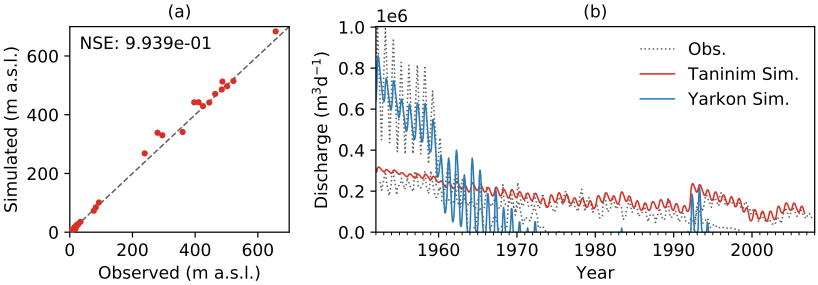

Computed vs. observed (a) steady-state well heads and (b) spring discharge.

Transient variably-saturated simulation (CPE-Model)

- Water levels well represented
- Only few data points in the mountainous regions

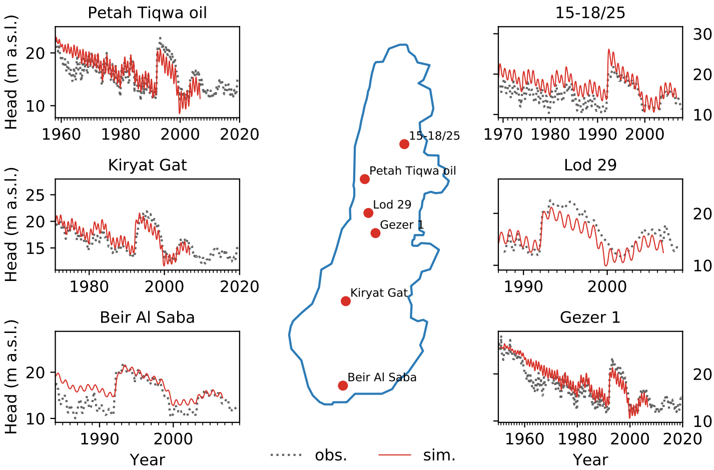

Small-scale process-oriented studies

- Simulation of infiltration through a synthetic solution doline
- Shape of the doline described via (Péntek et al., 2007):

$$\mu(x) = [\frac{1}{M} \ln \frac{x}{L}]^{\frac{1}{K}} \qquad (1)$$

$L > 0$: Parameter controlling the doline depth

$M < 0$: Parameter controlling the doline diameter

$K \leq 0$: Parameter controling the inflection point of the meridian curve

- Van-Genuchten Parameter of the primary continuum have a much greater impact for infiltration dynamics

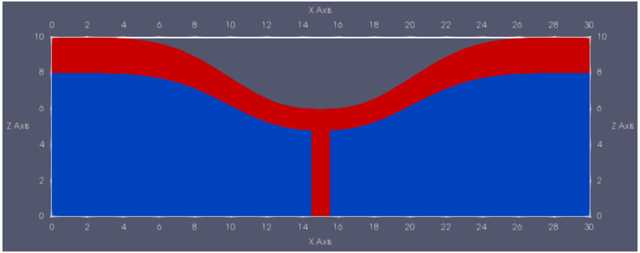

Model geometry of the doline. The red area indicates zones that have been discretized in a dual-continuum representation.

Small-scale process-oriented studies

- The volumetric fraction w_d of the second continuum has very little influence on the discharge
- Exchange flux mostly occurs along the capillary fringe.
- Under unsaturated conditions the matrix continuum has a lower matric potential.

$\Rightarrow$ Flow from matrix to conduit is mathematically impossible under unsaturated conditions (Van-Genuchten limitations).

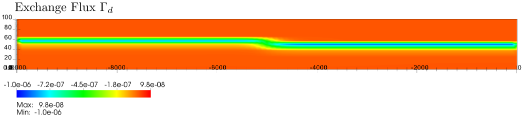

Matrix-Conduit exchange flux

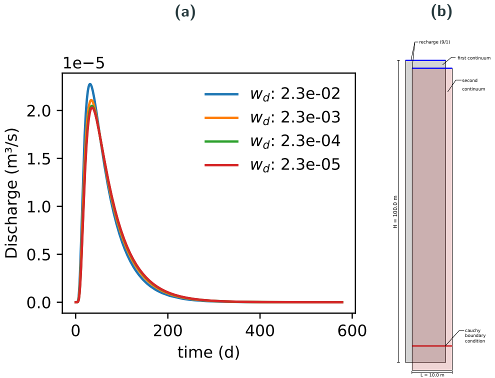

Testing the coupling of the two continua under unsaturated conditions via a simplified simulation.

- Synthetic dry valley
- Investigation of the parameters controlling the coupling of surface-subsurface flow

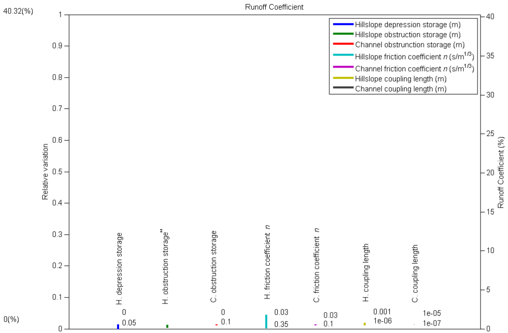

Influence of the different surface hydraulic parameters on the runoff coefficient.

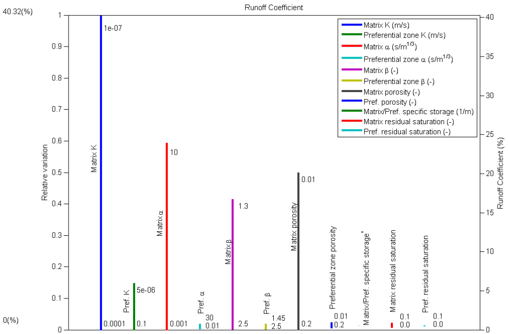

Influence of the different subsurface hydraulic parameters on the runoff coefficient.

Conclusion & Outlook

Conclusions:

- Variably-saturated dual-continuum flow models seem to not allow for unsaturated flow through the second continuum.
- Hydraulic properties of the near-surface subsurface strongly control the runoff coefficient.
- With increasing computational resources, integrated surface-subsurface flow models may provide useful tools to estimate event-based recharge.

Outlook:

- Currently, separately calculated monthly recharge rates from 1951 to 2006 are used in the model.
- In the long run, groundwater recharge shall be calculated by simulating overland flow and computing actual Evapotranspiration within HydroGeoSphere. This allows accounting for the partitioning of rainfall into surface runoff in a spatially and temporally distributed manner. The impact of climatic changes on infiltration dynamics shall be investigated as a next step.

Thank you for your attention – Questions?
Contact me via email (lbresin@gwdg.de) or join the live chat.

Supplementary Slides:
References
Appendix:
Appendix A: "Mathematical Framework of HGS"
Appendix B: "Geology and Palaeo-hydrogeology of the WMA"

GEORG-AUGUST-UNIVERSITÄT GÖTTINGEN

Technische Universität Berlin

Bundesministerium für Bildung und Forschung

GöHPC

MedWater

Fleischer, L. (2002). Stratigraphic Table of Israel: Outcrops and Subsurface. Technical report, Geophysical Institute of Israel.

Hartmann, A., Goldscheider, N., Wagener, T., Lange, J., and Weiler, M. (2014). Karst water resources in a changing world: Review of hydrological modeling approaches. *Reviews of Geophysics*, 52(3):218–242.

Kordilla, J., Noffz, T., Dentz, M., Geyer, T., and Tartakovsky, A. M. (2017). Effect of Unsaturated Flow Modes on Partitioning Dynamics of Gravity-Driven Flow at a Simple Fracture Intersection: Laboratory Study and Three-Dimensional Smoothed Particle Hydrodynamics Simulations. *Water Resources Research*, 53(11):9496–9518.

Mualem, Y. (1976). A new model for predicting the hydraulic conductivity of unsaturated porous media. *Water Resources Research*, 12(3):513–522.

Péntek, K., Veress, M., and Lóczy, D. (2007). A morphometric classification of solution dolines. *Zeitschrift fur Geomorphologie*, 51(1):19–30.

van Genuchten, M. T. (1980). A Closed-form Equation for Predicting the Hydraulic Conductivity of Unsaturated Soils. *Soil Science Society of America Journal*, 44(5):892–898.

Weinberger, G., Rosenthal, E., Ben-Zvi, A., and Zeitoun, D. (1994). The Yarkon-Taninim groundwater basin, Israel hydrogeology: case study and critical review. *Journal of Hydrology*, 161(1-4):227–255.

Zilberbrand, M., Rosenthal, E., and Weinberger, G. (2014). Natural tracers in Senonian-Eocene formations for detecting interconnection between aquifers. *Applied Geochemistry*, 47:157–169.

Appendix A.1: Mathematical Framework of HGS - Overview of the flow compartments

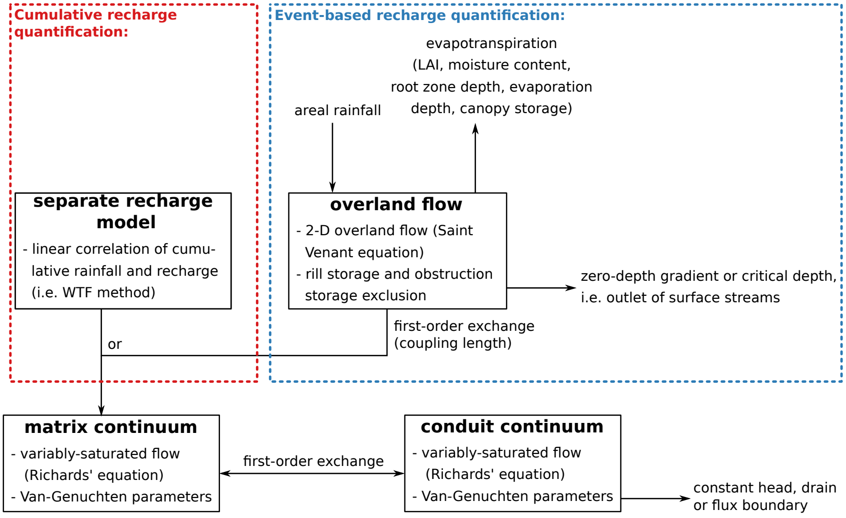

Simulation of various flow compartments with HGS

Appendix A.2: Mathematical Framework of HGS - Computation of flow

- 2D surface routing (Saint Venant):

$$-\nabla \cdot (d_o \boldsymbol{q_o}) - d_o \Gamma_o \pm Q_o = \frac{\partial \phi_o h_o}{\partial t}. \qquad (2)$$

where $\boldsymbol{q_o}$ is defined as: $\boldsymbol{q_o} = -\boldsymbol{K_o} \cdot k_{ro} \nabla (d_o + z_o)$

d_o: depth of flow ($h_o = z + d_o$)
ϕ_o: porosity (olf)
Γ_o: exchange term
K_o: obt. from Chezy, Manning or Darcy-Weisbach equation
k_{ro}: conductance reduction from obstruction storage exclusion

h_o: surface water head
Q_o: volumetric fluid flux (bcs)
$\boldsymbol{q_o}$: fluid flux

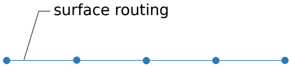

Framework of integrated multi-continuum models.

Appendix A.2: Mathematical Framework of HGS - Computation of flow

- Richards' equation (porous medium):

$$-\nabla \cdot (w_m \boldsymbol{q_m}) + \Gamma_o + \Gamma_d \pm Q_m = w_m \frac{\partial}{\partial t}(\theta_{sm} S_{wm}), \qquad (3)$$

where the fluid flux $\boldsymbol{q_m}$ is defined as: $\boldsymbol{q_m} = -\boldsymbol{K_m} \cdot k_{rm} \nabla(\psi_m + z_m)$.

w_m: volumetric fraction
Γ_o, Γ_d: exchange term
θ_{sm}: saturated water content
z_m: elevation head
S_{wm}: water saturation ($S_{wm} = \frac{\theta_m}{\theta_{sm}}$)
k_{rm}: relative conductivity (controls variably-saturated flow)

$\mathbf{q_m}$: fluid flux
Q_m: volumetric fluid flux (bcs)
$\mathbf{K_m}$: hydraulic conductivity
ψ_m: pressure head

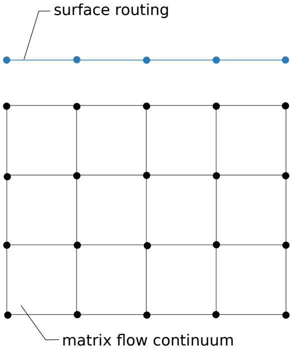

Framework of integrated multi-continuum models.

Appendix A.2: Mathematical Framework of HGS - Computation of flow

- Richards' equation (dual medium):

$$-\nabla \cdot (w_d \boldsymbol{q_d}) - \Gamma_d \pm Q_d = w_d \frac{\partial}{\partial t}(\theta_{sd} S_{wd}), \qquad (4)$$

where $\boldsymbol{q_d}$ is defined as: $\boldsymbol{q_d} = -\boldsymbol{K_d} \cdot k_{rd} \nabla(\psi_d + z_d)$.

w_d: volumetric fraction
Γ_d: exchange term
θ_{sd}: saturated water content
z_d: elevation head
S_{wd}: water saturation ($S_{wd} = \frac{\theta_d}{\theta_{sd}}$)
k_{rd}: relative conductivity (controls variably-saturated flow)

$\mathbf{q_d}$: fluid flux
Q_d: volumetric fluid flux (bcs)
$\mathbf{K_d}$: hydraulic conductivity
ψ_d: pressure head

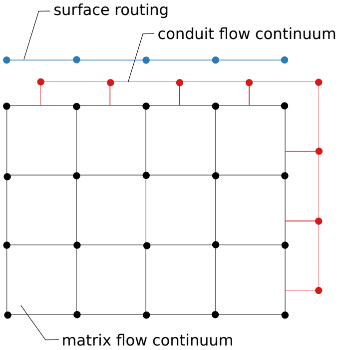

Framework of integrated multi-continuum models.

- Porous/dual medium coupling:

$$\Gamma_d = \frac{\beta_g}{a^2}\gamma_w K_\alpha k_{ra}(\psi_d - \psi_m). \qquad (5)$$

β_g: geometrical shape factor
γ_w: empirical coefficient
k_{ra}: relative hydraulic conductivity
a: skin thickness
ψ_d, ψ_m: pressure head
K_α: interface hydraulic conductivity

- Surface/subsurface coupling:

$$d_o\Gamma_o = w_m \frac{k_{rm}K_{zz}}{l_{ex}}(h_m - h_o) + w_d \frac{k_{rd}K_{dzz}}{l_{ex}}(h_d - h_o). \qquad (6)$$

h_m,h_d: hydraulic head
d_o: depth of flow ($h_o = z + d_o$)
k_{rm},k_{rd}: relative conductivity
K_{zz},K_{dzz}: vertical hydraulic conductivity
h_o: surface water head
w_m,w_d: volumetric fraction
l_{ex}: coupling length

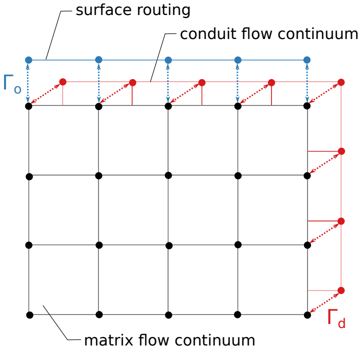

Framework of integrated multi-continuum models.

Appendix A.2: Mathematical Framework of HGS - Van-Genuchten parameterization

- Nonlinear dependence of $k_r(S_w)$ and $S_w(\Psi)$ (Mualem, 1976; van Genuchten, 1980):

$$k_r = {S_e}^{l_p}(1-(1-{S_e}^{\nu^{-1}})^{\nu})^2, \tag{7}$$

$$S_e = \frac{S_w - S_{wr}}{1 - S_{wr}}, \tag{8}$$

$$S_w = S_{wr} + (1-S_{wr})[1+|\alpha\psi|^{\beta}]^{-\nu}, \text{for } \psi < 0, \tag{9}$$

where $\nu = 1 - \frac{1}{\beta}$, $\beta > 1$.

S_e: effective saturation
S_{wr}: residual saturation
α: inverse air-entry pressure head
S_w: saturation ($S = \frac{\theta}{\theta_s}$)
l_p: pore-connectivity parameter
β: pore-size distribution index

- Prone to degeneracy.
- Hysteresis is not considered here.

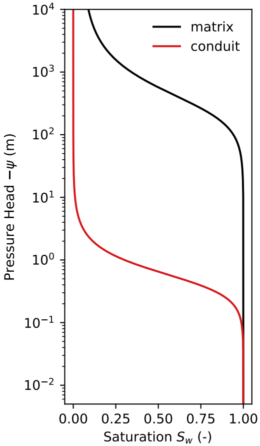

Water retention curve.

Appendix A.2: Mathematical Framework of HGS - Subtime Stepping

- Time step size is a key factor in controlling the model accuracy and efficiency
- Implicit sub-time stepping approach:

$$\Delta t^{L+1} = \frac{X_{max}}{\max |X_i^{L+1} - X_i^L|} \Delta t^L \tag{10}$$

X: value of the time-controlling variable at node i
L: current time level
X_{max}: defined maximum change of variable X
Δt: time step

where the variable X can be the hydraulic head and/or saturation.

Appendix B.1: Geology and Palaeo-hydrogeology of the WMA - Stratigraphic column

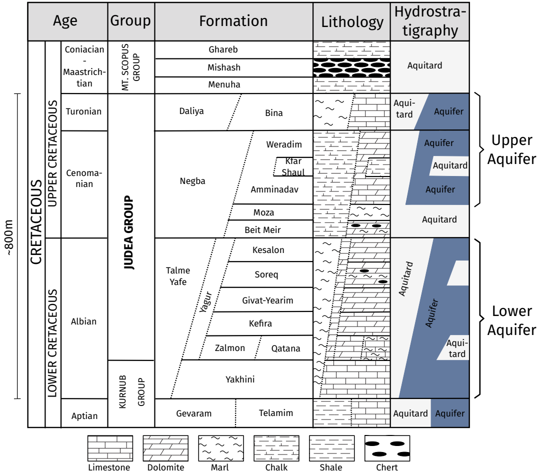

Stratigraphic and hydrostratigraphic column from West to East (modified after Fleischer, 2002; Weinberger et al., 1994; Zilberbrand et al., 2014)

Appendix B.2: Geology and Palaeo-hydrogeology of the WMA - Development of karst voids

- Regional uplift (Oligiocene) of the Judaean mountians
  - Regression of the Tethys Sea
  - Formation of deep canyons along the coastline
  - $\Rightarrow$ Increased density of conduits in the proximity to paleo-canyons
- Lowering of the Mediterranean sea level
  - Messinian Salinity Crisis ($\sim 6\,\mathrm{Ma}$, Late Miocene) over a period of $\sim 0.6\,\mathrm{Ma}$
  - $\Rightarrow$ Lowering of the base-level
  - $\Rightarrow$ Development of karst conduits at great depth